Electronic Supplementary Material (ESI) for Soft Matter.

A Novel Nematic-Like Mesophase Induced in Dimers, Trimers and Tetramers Doped with a High Helical Twisting Power Additive

Richard J. Mandle and John W. Goodby

Supplementary Information

1. Experimental Methods

1.1. General Techniques

The synthesis of all materials used in this study has been described in previous publications: RM1041; [33] CB9CB, CBCC6OCB and CB8OCB; [34] $T_3$9; [35] $T_4$9; [35, 36]; $A6_3$; [37] $O4_7$. [38] All binary mixtures were prepared with 10 wt% of RM1041 and 90 wt% of the host material. Binary mixtures were prepared by weighing out the two components into separate vials to an accuracy of ±0.01 mg. The two components were dissolved into DCM, combined, and mixed with sonication before drying under a stream of N_2 gas with gentle warming.

1.2. Polarised Optical Microscopy

Polarised optical microscopy was performed on a Zeiss Axioskop 40Pol microscope using a Mettler FP82HT hotstage controlled by a Mettler FP90 central processor. Photomicrographs were captured *via* an InfinityX-21 MP digital camera mounted atop the microscope.

1.3. Differential Scanning Calorimetry.

Differential scanning calorimetry was performed on a Mettler DSC822^e fitted with an autosampler operating with Mettler Star^e software and calibrated before use against an indium standard (onset = 156.55 ± 0.2 °C, ΔH = 28.45 ± 0.40 Jg^{-1}) under an atmosphere of dry nitrogen.

1.4. Small Angle X-ray Scattering

Small angle X-ray scattering was performed using a Bruker D8 Discover equipped with a temperature controlled, bored graphite rod furnace, custom built at the University of York. The radiation used was copper Kα (λ = 0.154056 nm) from a 1 μS microfocus source. Diffraction patterns were recorded on a 2048x2048 pixel Bruker VANTEC 500 area detector set at a distance of 121 mm from the sample. Samples were filled into 1mm capillary tubes and aligned with a pair of 1T magnets, with the field strength at the sample position being approximately 0.6T Diffraction patterns were collected as a function of temperature and the data processed using Matlab as follows. Two-dimensional scattering patterns were collected on cooling from the isotropic liquid until crystallisation in ~ 1.2 °C intervals with a temperature accuracy of +/- 0.1 °C. 2D SAXS patterns were radially averaged (0.05 ° step size) to give scattered intensity as a function of 2θ for each frame.

1.5. Computational Chemistry

Quantum chemical calculations were performed using the Gaussian 09 revision e.01 suite of programmes. [2] Gaussian output files were rendered in Qutemol. [40]

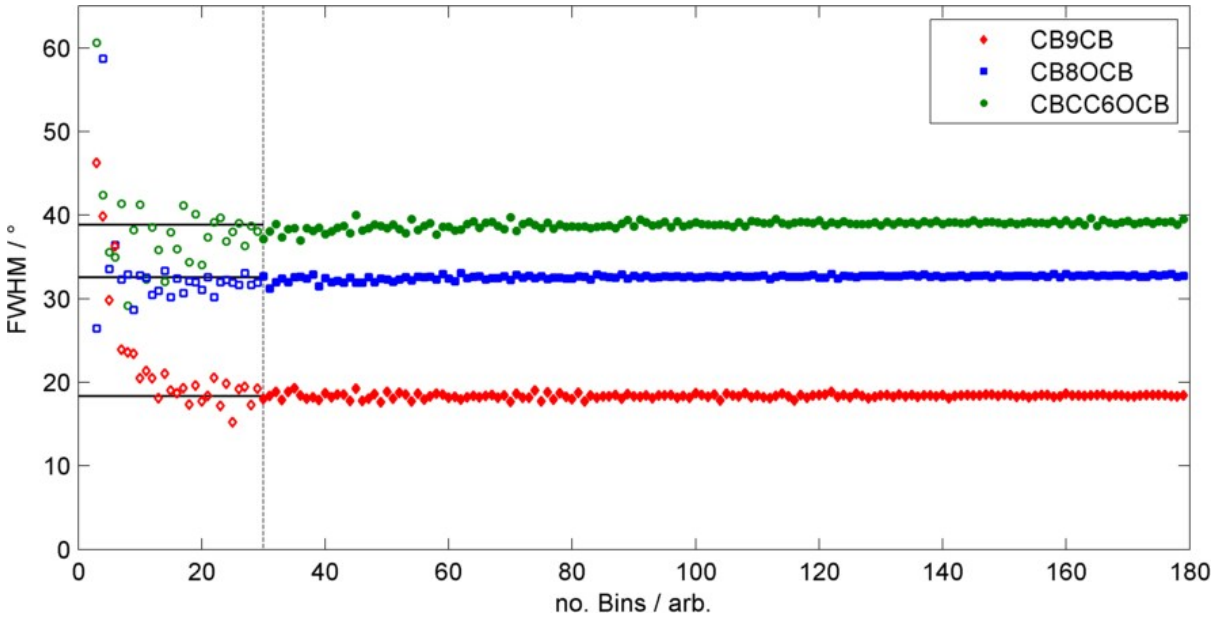

Figure SI-1: Plot of the FWHM (°) of a Gaussian fit to the histogram plot of bend-angle probability as a function of the number of bins. The FWHM values quoted in the text are taken as the mean of all values where the number of bins is between 30 and 180. The dashed vertical line indicates this cut off number of bins, while the solid horizontal lines show the FWHM values for all three materials. Data points coloured solid count towards the mean FWHM, hollow data points do not.

2. Detailed Host Information

2.1. Tabulated Transitional Data

No.		MP	SmA – Iso	TB – N	N - Iso
RM1041	**T**	141.7	137.6	-	-
	ΔH	32.6	2.4	-	-
CBCC6OCB	**T**	137.1	-	102.0	153.6
	ΔH	35.8	-	<0.1	1.6
CB9CB	**T**	83.3	-	105.4	121.5
	ΔH	29.2	-	0.6	2.0
CB8OCB	**T**	110.6	-	109.9	153.3
	ΔH	33.9	-	<0.1	2.3
$A6_3$	**T**	140.9	-	133.3	170.9
	ΔH	30.0	-	1.0	2.0
$T3_9$	**T**	146.5	-	164.2	210.3
	ΔH	41.6	-	0.3	2.6
$T4_9$	**T**	113.6	-	127.7	141.5
	ΔH	51.0	-	3.4	3.1

Table 1: Transition temperatures (T, °C) associated enthalpies (ΔH, kJ mol^{-1}) for mixtures **2** and **3** the components (**A**, **B**). Values were determined by DSC at a heat/cool rate of 10 °C min^{-1}. N = nematic, N * = chiral nematic, TB = twist-bend phase, SmA = smectic A.

2.2. Molecular Structures of Hosts

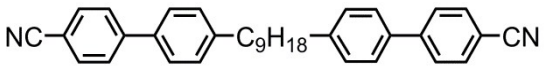

Figure SI-2: The chemical structure of CB9CB (**1**)

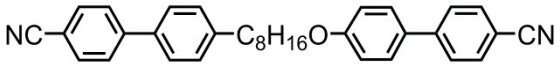

Figure SI-3: The chemical structure of CB8OCB (**2**)

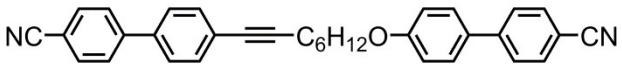

Figure SI-4: The chemical structure of CBCC6OCB (**3**)

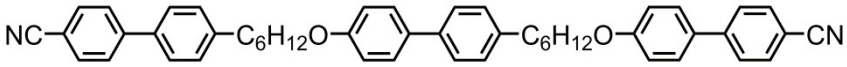

Figure SI-5: The chemical structure of $A6_3$ (**4**)

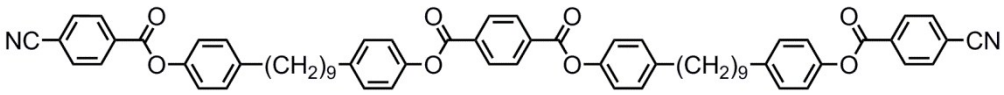

Figure SI-6: The chemical structure of $T3_9$ (**5**)

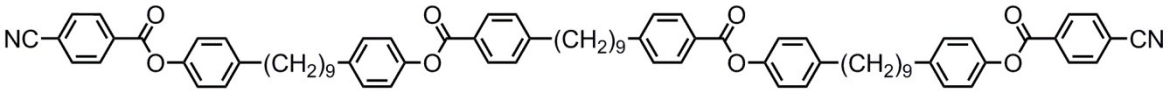

Figure SI-7: The chemical structure of $T4_9$ (**6**)

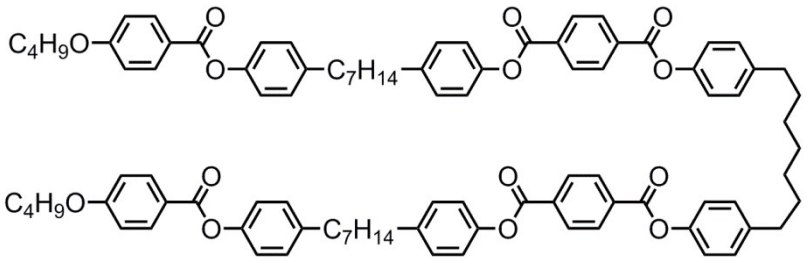

Figure SI-8: The chemical structure of $O4_7$ (**7**)

3. Chiral Dopant Information

We measured the helical twisting power (HTP) of the chiral dopant RM1041 *via* the Cano-Wedge method. We measure a HTP value of 88±1.4 μm^{-1}.

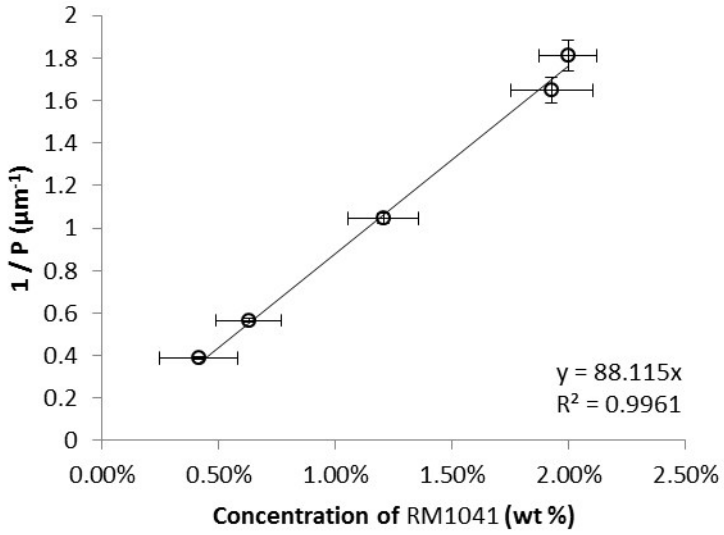

Figure SI-9: Plot of 1 / P (μm^{-1}) versus concentration (wt%) for binary mixtures of the chiral dopant RM1041 in 5CB. Linear fitting gives the helical twisting power (HTP) from the slope.

4. Supplementary POM Images

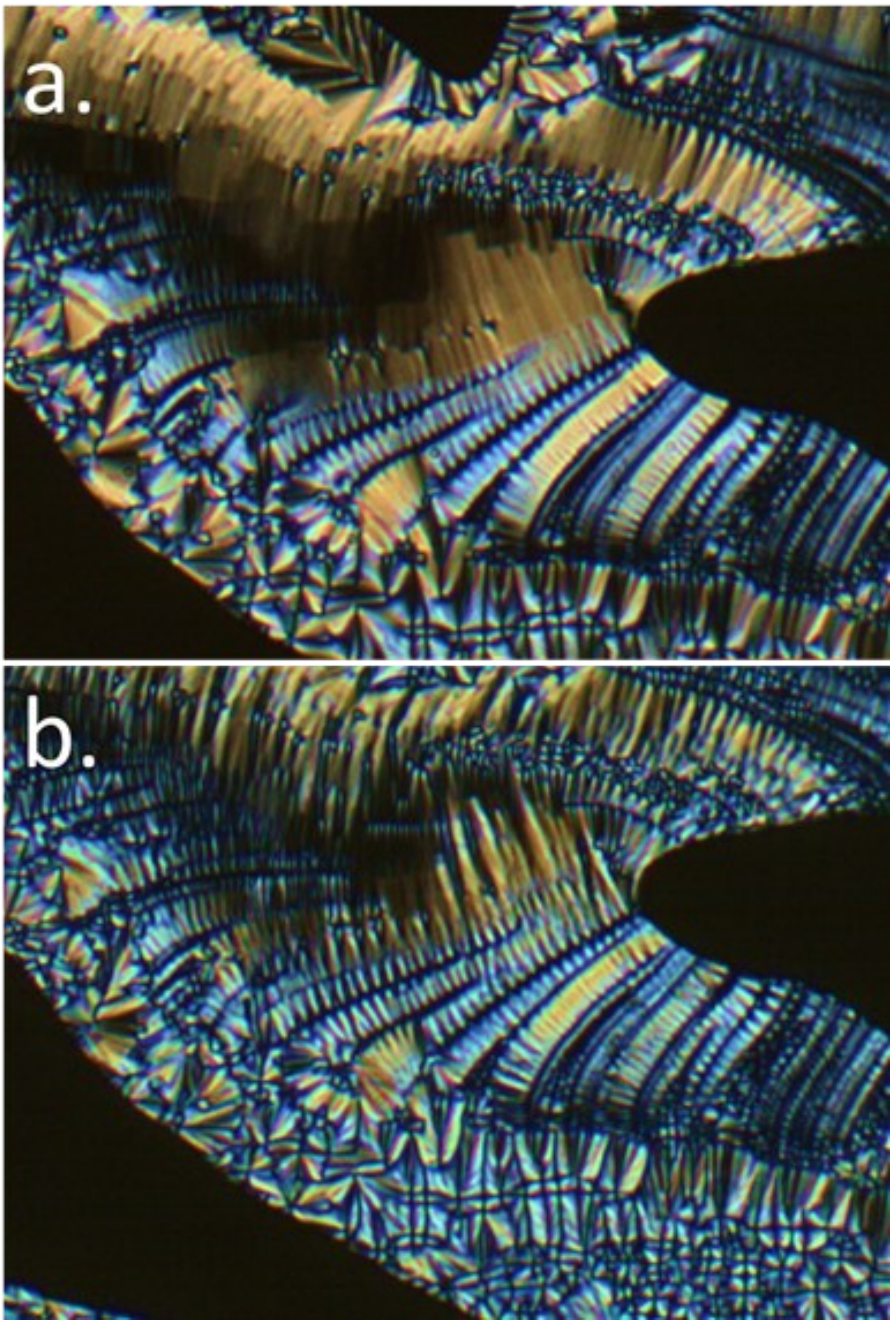

Figure SI-10: Photomicrographs of **3Mix** : The blocky texture of the TB phase (a, 92.1 °C) transforms into a blocky array of small parabolic defects in the N_X phase (b, 75 °C). Both photomicrographs are of approximately the same area of the sample.

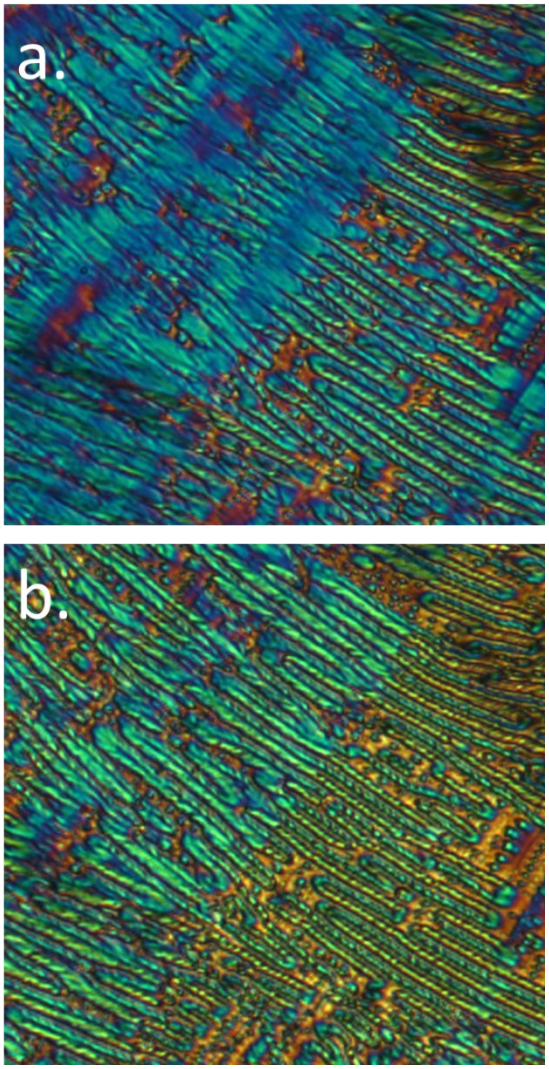

Figure SI-11: Photomicrographs of **5Mix** : The rope-like texture of the TB phase (a, 139.0 °C) and a rope-like texture in the N_X phase (b, 126.0 °C). Both photomicrographs are of approximately the same area of the sample.

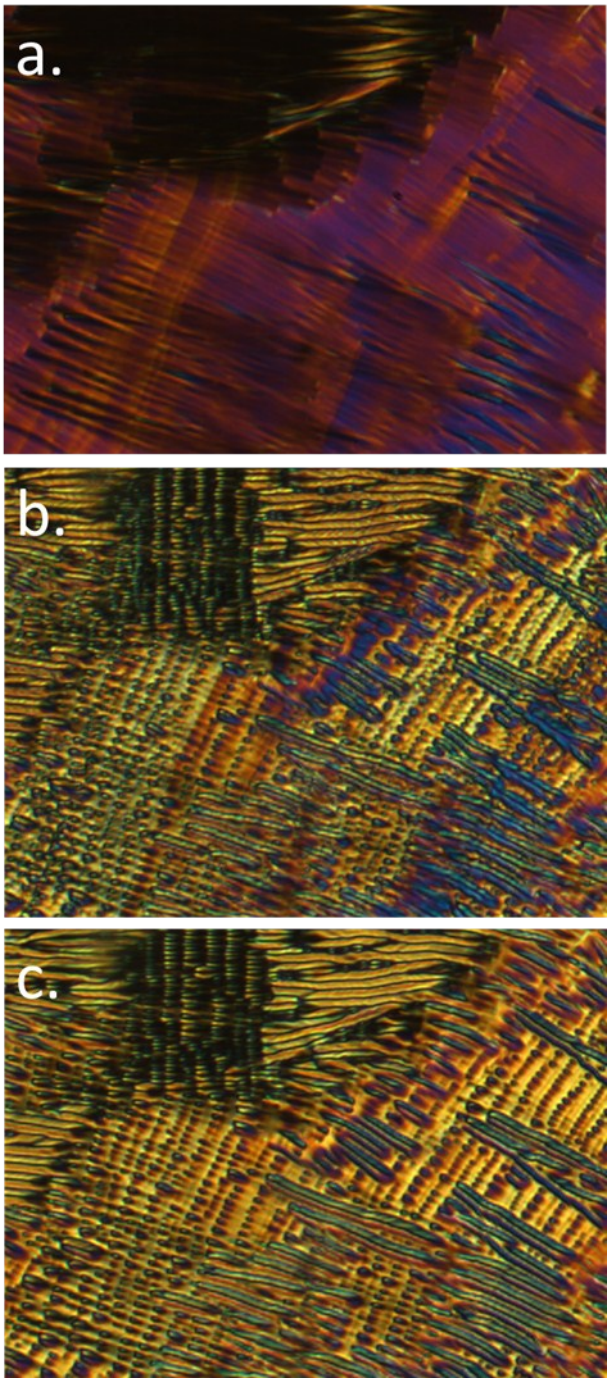

Figure SI-12: Photomicrographs of **6Mix** : The blocky texture of the TB phase (a, 103.0 °C) gives way to a rope-like texture (b, 93.3 °C) which persists on cooling into the N_X phase albeit with a change in birefringence (c, 86.0 °C). All three photomicrographs are of approximately the same area of the sample.

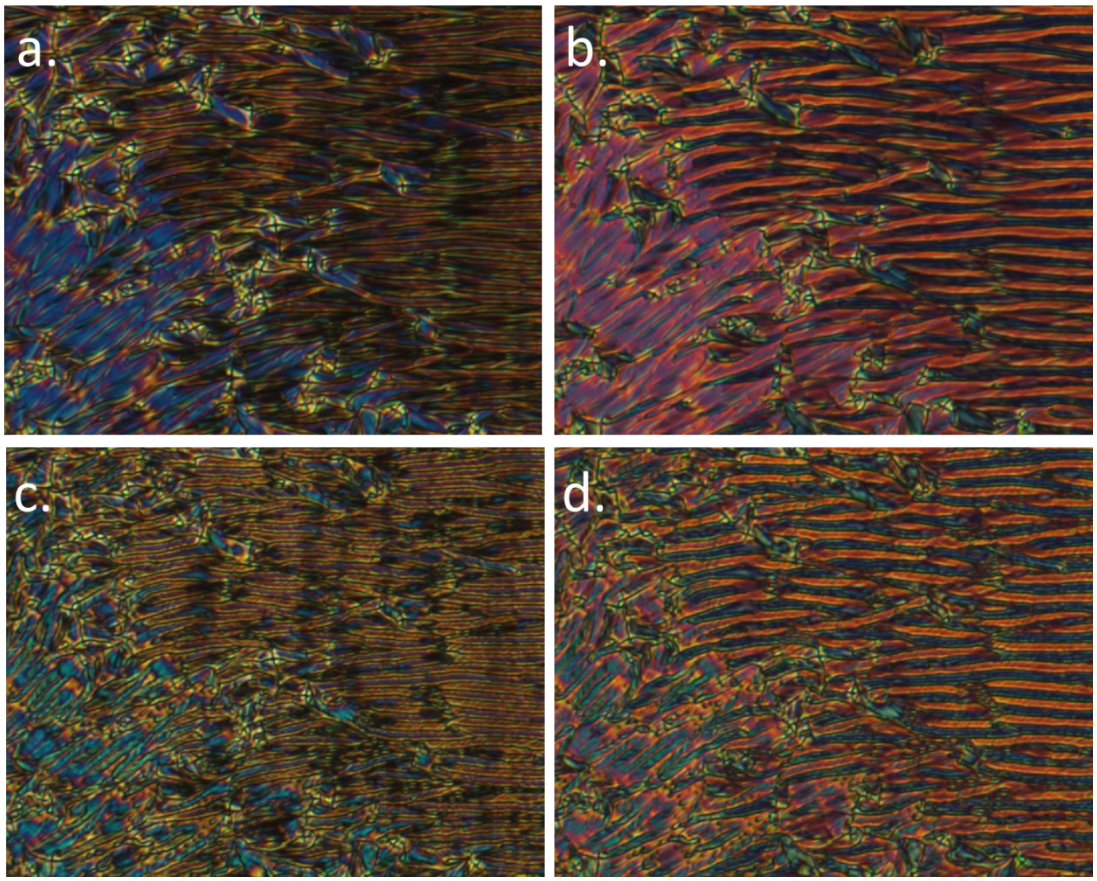

Figure SI-13: Photomicrographs of **7Mix**: The focal-conic and rope-like textures of the TB phase (a, 150.0 °C), and with a ¼ waveplate inserted (b, 150 °C). focal-conic and rope-like textures of the N_X phase (c, 122.0 °C) and with a ¼ waveplate inserted (d, 122.0 °C).

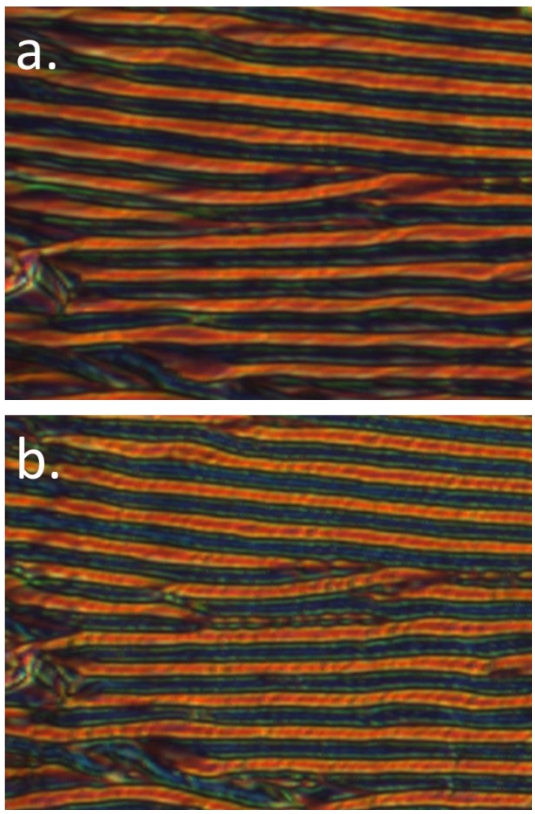

Figure SI-14: Photomicrographs of the rope-like texture of **7Mix** in the TB phase (a, 150.0 °C) with a ¼ waveplate inserted, and in the N_X phase (c, 122.0 °C) with a ¼ waveplate inserted.

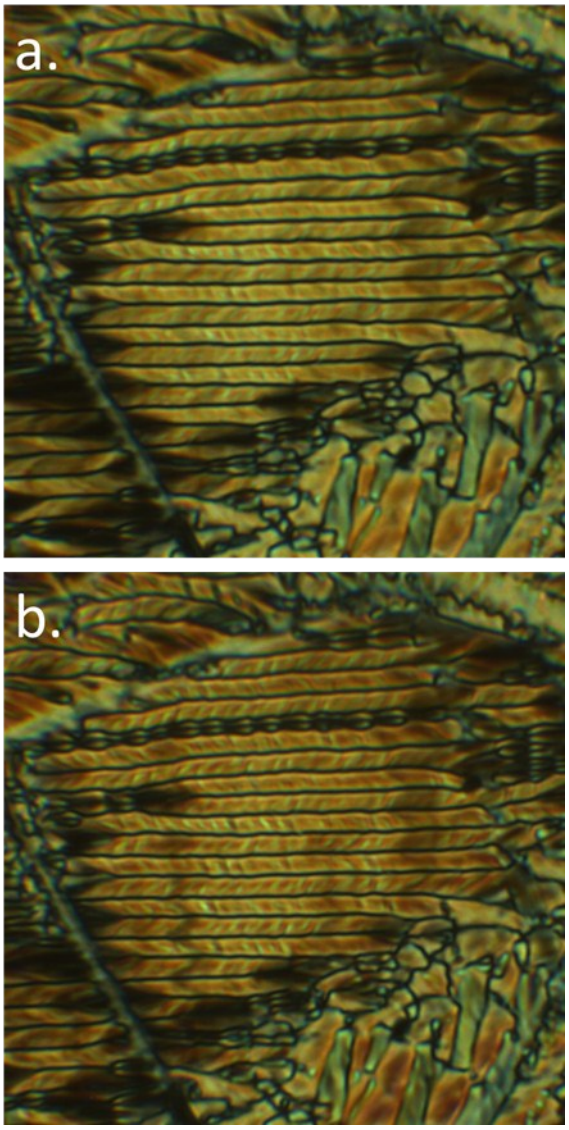

Figure SI-15: Photomicrographs of the rope-texture of (a) the TB phase of **M10** at 72 °C, (b) the rope texture of the N_X phase of **M10** at 62 °C. Note the small change in birefringence. Both photomicrographs are of approximately the same area of the sample.

5. Supplementary DSC Data

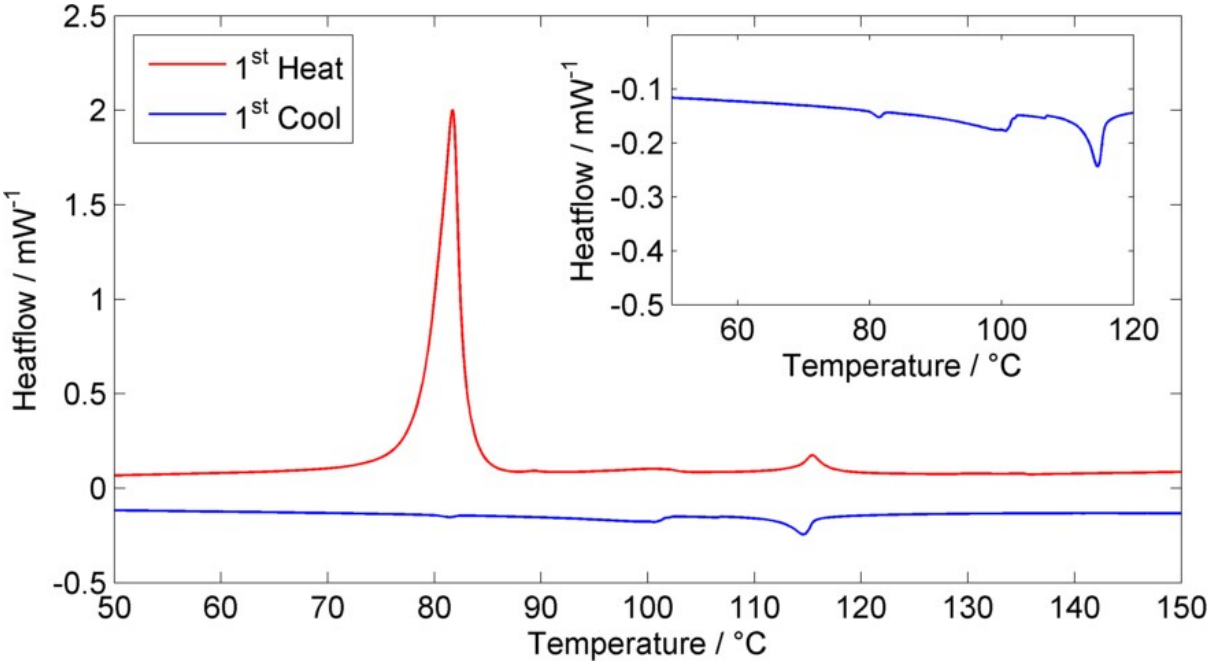

Figure SI-16: DSC trace (10 °C min^{-1}) obtained for **1Mix** (90% CB9CB + 10 % RM1041), with an expansion showing the Iso-N*, N*-TB and TB-N_X phase transitions.

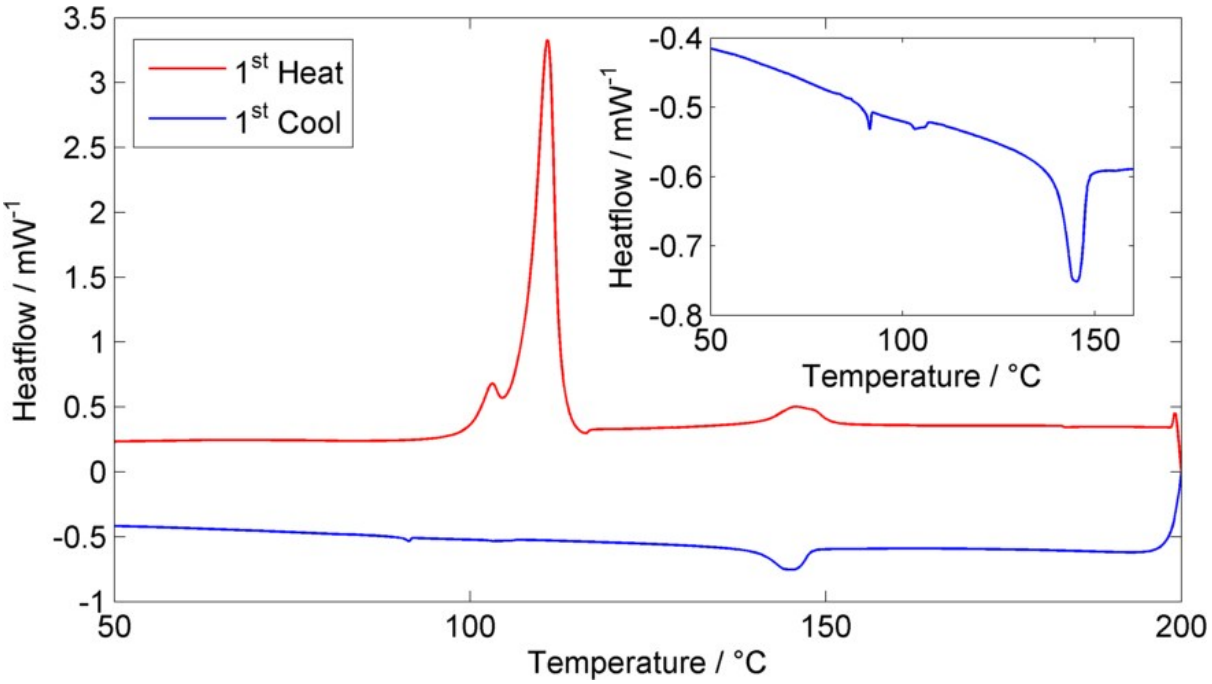

Figure SI-17: DSC trace (10 °C min^{-1}) obtained for **2Mix** (90% CB8OCB + 10 % RM1041), with an expansion showing the Iso-N*, N*-TB and TB-N_X phase transitions.

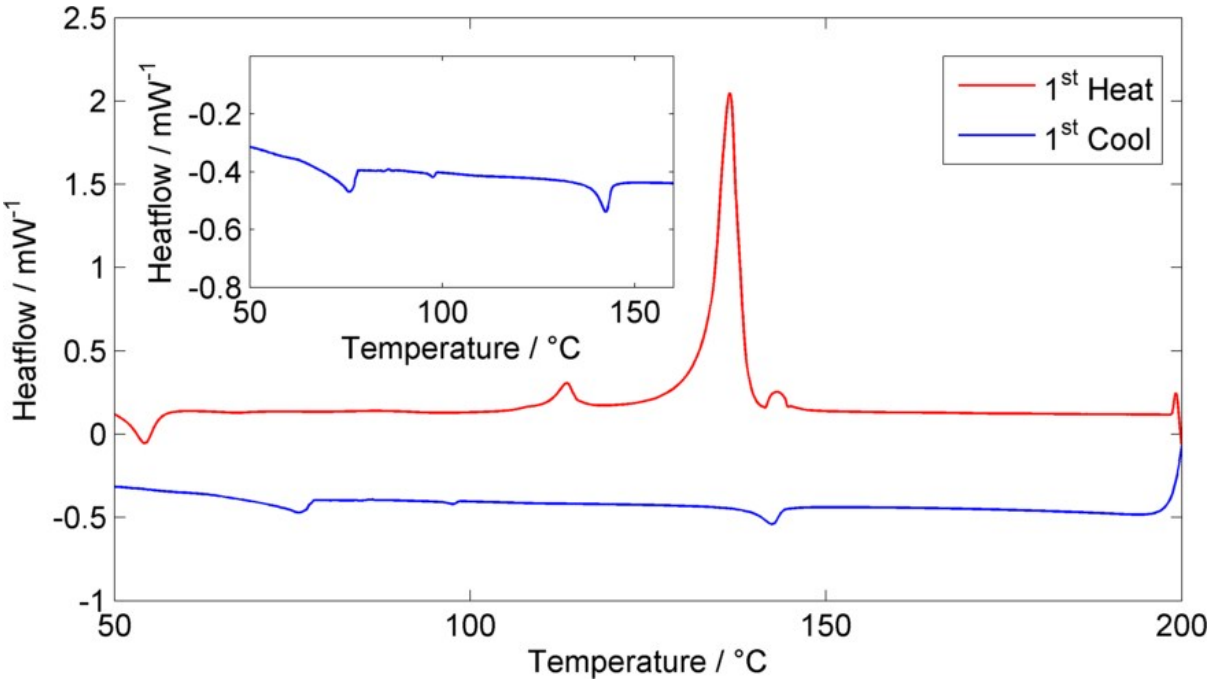

Figure SI-18: DSC trace (10 °C min^{-1}) obtained for **3Mix** (90% CBCC6OCB + 10 % RM1041), with an expansion showing the Iso-N*, N*-TB and TB-N_X phase transitions.

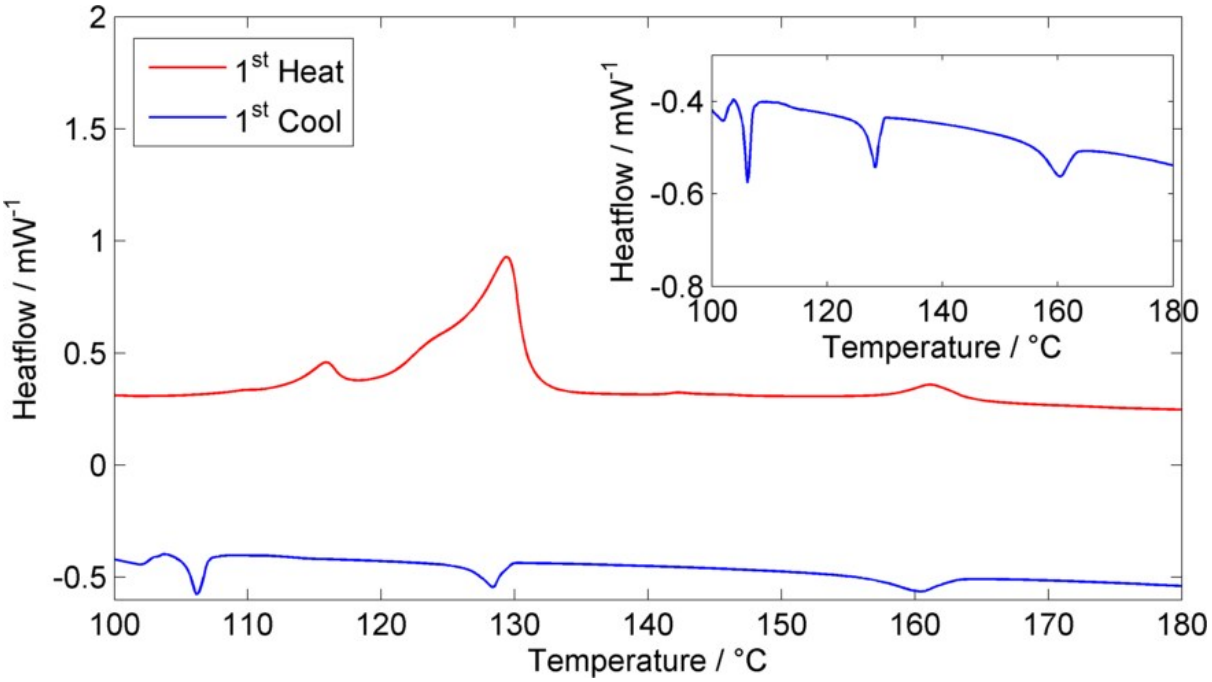

Figure SI-19: DSC trace (10 °C min^{-1}) obtained for **4Mix** (90% $A6_3$ + 10 % RM1041), with an expansion showing the Iso-N*, N*-TB and TB-N_X phase transitions.

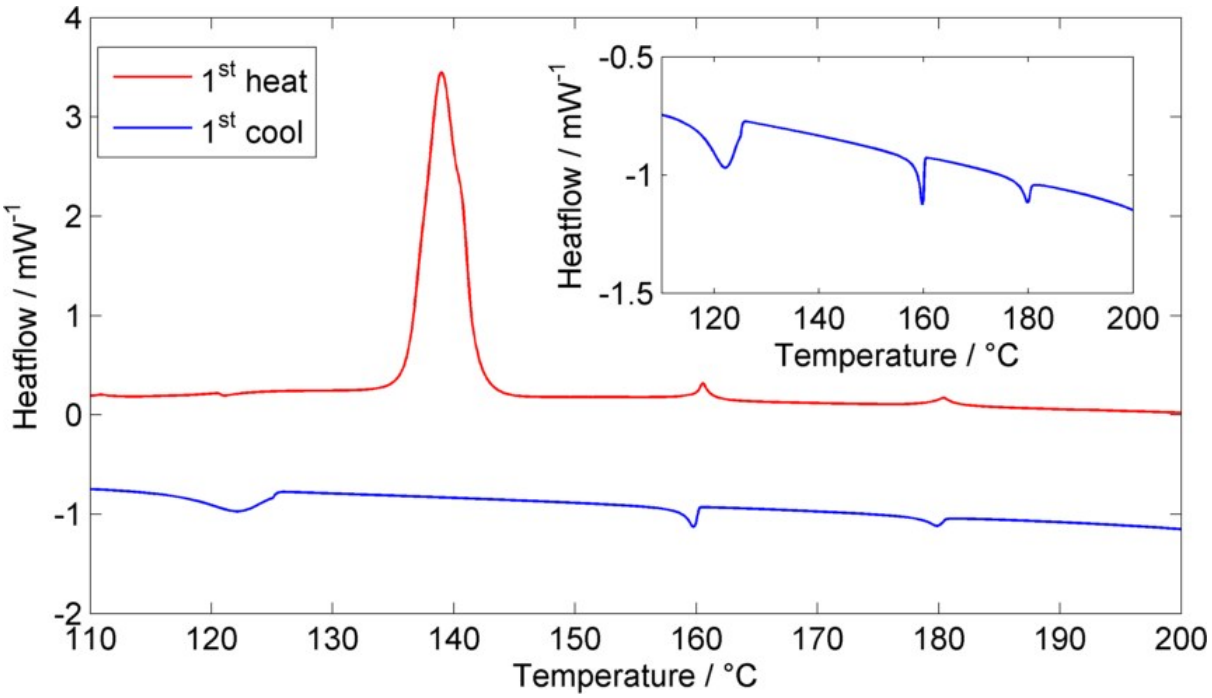

Figure SI-20: DSC trace (10 °C min^{-1}) obtained for **7Mix** (90% $O4_7$ + 10 % RM1041), with an expansion showing the Iso-N*, N*-TB and TB-N_X phase transitions.